OXFORD

Cerebral Cortex, 2016; 1–11

doi: 10.1093/cercor/bhw313
Original Article

ORIGINAL ARTICLE

Illusory Obesity Triggers Body Dissatisfaction Responses in the Insula and Anterior Cingulate Cortex

Catherine Preston[1,2] and H. Henrik Ehrsson[1]

[1]Department of Neuroscience, Karolinska Institutet, Stockholm 17177, Sweden and [2]Psychology Department, University of York, York YO10 5DD, UK

Address correspondence to Catherine Preston, Psychology Department, University of York, York YO10 5DD, UK. Email: catherine.preston@york.ac.uk

Abstract

In today's Western society, concerns regarding body size and negative feelings toward one's body are all too common. However, little is known about the neural mechanisms underlying negative feelings toward the body and how they relate to body perception and eating-disorder pathology. Here, we used multisensory illusions to elicit illusory ownership of obese and slim bodies during functional magnetic resonance imaging. The results implicate the anterior insula and the anterior cingulate cortex in the development of negative feelings toward the body through functional interactions with the posterior parietal cortex, which mediates perceived obesity. Moreover, cingulate neural responses were modulated by nonclinical eating-disorder psychopathology and were attenuated in females. These results reveal how perceptual and affective body representations interact in the human brain and may help explain the neurobiological underpinnings of eating-disorder vulnerability in women.

Key words: body perception, body satisfaction, emotion, fMRI, multisensory body illusions

Introduction

Imagine the feeling when, packing for your dream holiday, you try on last year's beachwear only to discover that you have put on more weight than you thought, or when trying on an old favorite pair of jeans, you can no longer fasten the top button. Negative feelings toward our body are easily evoked, especially in today's developed world, where concerns about body size are becoming a widespread obsession. A person's negative thoughts and feelings about his or her body is also known as body dissatisfaction (Grogan, 2008). Body dissatisfaction is thought to not only be detrimental for general well-being but is also implicated in the development and maintenance of eating disorders, such as anorexia and bulimia nervosa (Stice and Shaw 2002), which primarily affect young women (Fairburn and Harrison 2003). Women, who make up the vast majority of patients clinically diagnosed with eating disorders, are found to have higher rates of body dissatisfaction in the healthy population compared with men (Pingitore et al. 1997; Lawler and Nixon 2011). Thus, this susceptibility to body dissatisfaction may be an important factor underlying the higher rates of eating disorders in women.

Historically, eating disorders such as anorexia were thought to have a social origin and, indeed, social pressures differ for men and women, particularly in terms of the importance of physical appearance. However, it has also been suggested that those with eating disorders, particularly anorexia nervosa, have a deficit in body perception. Many studies have shown anorexia patients to overestimate their body size (Slade and Russell 1973; Smeets 1999; Keizer et al. 2011, 2013), although this phenomenon is still disputed (Cornelissen et al. 2013). However, we do know that experimental modulation of perceived body size has a direct effect on body satisfaction in healthy individuals (Preston and Ehrsson 2014). Thus, it is possible that any distortions of body size perception observed in anorexia patients may be linked to their low levels of body satisfaction. However, because these questions are difficult to clarify in patient populations there is a need for well-controlled experimental studies in healthy

participants that examine the fundamental link between body perception and body satisfaction.

The neural networks involved in body perception are well known, and these include the posterior parietal and premotor brain regions responsible for multisensory integration, which allow for maintenance and updating of the perceptual representation of the body in the brain (Graziano 1999; Ehrsson et al. 2004; Gentile et al. 2011; Petkova et al. 2011; Limanowski and Blankenburg 2015). The parietal lobes have also been linked to anorexia nervosa, suggesting that deficits in this region are responsible for abnormal experiences of body perception (Wagner et al. 2003; Castellini et al. 2013). Currently, much less is known about the neural correlates of body satisfaction. However, the anterior insula and anterior cingulate cortex are 2 regions implicated in emotional processing (Bush et al. 2000; Damasio et al. 2000) and are thought to be key nodes in the brain circuitry mediating interoceptive awareness and in monitoring the physiological state of the body (Craig 2002). Moreover, the anterior cingulate cortex is found to have reduced gray matter volume (Joos et al. 2011) and blood perfusion (Naruo et al. 2001) in anorexic patients, and the anterior insula has been linked to body anxiety and is found to have greater activity during a body comparison task in anorexia patients compared with controls (Friederich et al. 2010). Thus, these regions are prime candidates for an "affective body representation," which may be important in the development of eating disorders. However, direct evidence for this is lacking, as well as evidence of neural links to body perception networks. Moreover, by definition, anorexia patients are severely underweight, which means that it is unclear whether any observed neural abnormalities in these patients have a causal role in eating-disorder pathology or are purely a consequence of starvation (Frank 2013).

In this study, we aimed to examine the neural correlates of body satisfaction in healthy controls and possible links to perceptual body representation networks using a multisensory body illusion that elicits the illusory experience of being obese. The resultant neural activity was also related to nonclinical levels of eating-disorder psychopathology to determine if the link with eating-disorder psychopathology remains without the confounds of dehydration and emaciation found with clinical patients.

Multisensory full-body illusions (Petkova and Ehrsson 2008) were used to induce illusory ownership of both slim and obese bodies while recording subjective body satisfaction and neural responses using functional magnetic resonance imaging (fMRI). Multisensory illusions can be used to modulate perceived body size (Ehrsson, Kito, et al. 2005; Normand et al. 2011), which can directly influence body satisfaction in healthy individuals (Preston and Ehrsson 2014). For the present illusions, we delivered touches to the body of either a slim or obese stranger viewed by a participant from a natural perspective via prerecorded videos presented through MR-compatible head-mounted displays (HMDs). At the same time, we applied synchronous touches to the participant's unseen real body. This procedure elicits a vivid illusion that the stranger's body is your own and that the touches you see are the same as those you feel (Petkova and Ehrsson 2008). Asynchronous touch abolishes the illusion and provides a control for otherwise equivalent conditions.

We hypothesized that body dissatisfaction triggered by illusory obesity would be associated with activation of the anterior insula cortex and the anterior cingulate cortex. We also hypothesized that such affective responses would be driven by functional interactions with areas in the posterior parietal cortex involved in body perception (Ehrsson et al. 2004; Petkova et al. 2011; Guterstam, Björnsdotter, et al. 2015). In addition, because eating disorders and body dissatisfaction are more common in women than in men, we sought to explore sex-related differences in behavioral and neural responses to illusory obesity.

Materials and Methods

Participants

Thirty-two healthy participants (16 males, 16 females) were recruited for the experiment. To control for possible confounding variables that may influence body satisfaction, additional measures, and screening were completed for this sample similar to those outlined by a previous experiment (Preston and Ehrsson 2014). Participants were screened for current psychiatric conditions using the Mini International Neuropsychiatric Interview screen (Lecrubier et al. 1997) and for eating-disorder psychopathology using the Eating Disorder Examination Questionnaire (EDE-Q) (see below). A global score of 2.8 was used as a clinical cut-off for the EDE-Q (Mond et al. 2008). The participants were also asked to confirm that they had no previous history of psychiatric or neurological disorders. To ensure that the participants' actual body sizes fell between that of the slim and obese sex-matched models, they were required to provide weight and height information during the screening process. Their weight was also checked when they arrived for the experiment. The participants were also screened for contradiction to MRI prior to taking part in the experiment. There were no significant differences between the male and female participants for any of the measures taken, although EDE-Q scores approached significance, with females tending to have higher scores compared with males (see Table 1). All participants gave informed consent to take part in the fMRI. The experiment was conducted in accordance with the Declaration of Helsinki and was approved by the Swedish Central Ethical Review Board.

Prerecorded Video Stimuli

To present images of realistic slim and obese bodies, prerecorded videos were produced by filming the bodies of real (slim and obese) models from a first-person perspective. The models were recruited through local advertisements and selected based on body mass index (BMI) and physical build. The slim male model had a muscular physique and a BMI of 20.4, and the obese male model had a BMI of 36. The slim female model was selected purely on body size and had a BMI of 18.4, and the obese female model had a BMI of 32.3. During filming, the models were asked to lie down on a bed with their arms by their sides, and 2 identical cameras (CamOne Infinity HD, resolution 1920 × 1080, Touratech AG) were placed just above their eyes,

Table 1 Participant demographics: means and (standard deviations)

Measure	Total mean	Male mean	Female mean	T statistic	P value
Age	25 (3.9)	25 (3.4)	25 (4.6)	0.264	0.79
BMI	22.9 (2.9)	23.6 (1.9)	22.2 (3.6)	1.34	0.19
SE[a]	24.0 (4.2)	25.0 (3.9)	23.0 (4.3)	1.65[b]	0.100[b]
EDE-Q	0.39[c] (0.65)	0.20[c] (0.32)	1.03[c] (0.76)	1.9[b]	0.061[b]

[a]Data missing for 3 participants.
[b]Mann–Whitney *U*-statistic.
[c]Median.
Abbreviations: SE, self-esteem; BMI, body mass index; EDE-Q, eating disorder examination questionnaire score (eating disorder psychopathology).

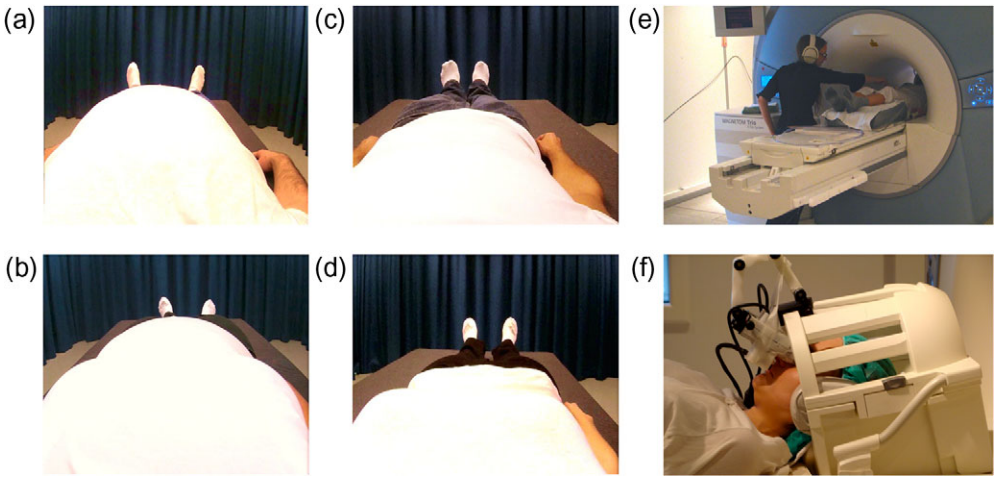

Figure 1. Experimental stimuli and set-up: Still images from videos of obese male (*a*), obese female (*b*), slim male (*c*), and slim female (*d*) bodies, which were presented to participants as they lay in the scanner bed. Touches were delivered to each participant in the scanner (*e*) while their head was tilted as if they were looking at their own body through the HMD (*f*).

pointing down at their body. The experimenter then used a stick (300 mm in length) attached to a white polystyrene sphere (30 mm diameter) to deliver tactile stimuli to the models' torsos. The 2 videos were then synchronized using Final Cut Pro 7 (Apple) with the recordings from the left and right cameras (which corresponded to the viewpoints of the left and right eyes, respectively) placed side-by-side in a single frame (1600 × 600 pixels) that corresponded to the display in the MR-compatible, HMDs. Using a frame-sequential technique implemented with custom-made hardware and BINO (http://bino3d.org) software, the videos were presented to the participants through the HMDs during the experimental brain imaging sessions, thus creating true stereoscopic, high-quality, 3D images of the different body types (Fig. 1). The timing of the touches in the videos was controlled by audio cues played to the experimenter during filming. The same audio track also cued the experimenter as to when to deliver the touches to the participants during the experiment and was either synchronized with the video images or delayed by 1000 ms to create synchronous and asynchronous trials, respectively. During the experiment, the audio cues were played to the experimenter via headphones to ensure that the participants could not hear them.

Procedure

During the experiment, the participants lay with their heads tilted (ca. 25°) on the bed of an MR scanner in a manner that was adopted from Petkova et al. (2011). For each participant, the MR-compatible HMD (Nordic Neurolab) was positioned in front of their eyes to present the videos of the different body types (Fig. 1). Each trial lasted 30 s and contained 18 touches that were equally divided between the left, right, and center of the torso. Each touch covered approximately 5 cm of the body, and the touches were delivered at approximately 10 cm/s (500 ms per touch). For each scan, there were 3 blocks of 4 trials (one of each of the 4 conditions, as described in the above: obese synchronous, obese asynchronous, slim synchronous, and slim asynchronous), alternating between synchronous and asynchronous conditions. The order of the trial types was counterbalanced both within and between participants. After each trial, 2 questions were presented through the HMDs. The first question assessed how the participant felt about their body at that moment in time ("Right now, how satisfied are you with your body?"), and the second question asked participants to indicate their level of agreement with an ownership statement ("The body in the image felt like it was my body"). The body satisfaction question was also presented at the beginning of each scan run to collect a baseline measure. The presentation of the first question was followed by a 3 s fixation period (fixation cross) before the trials began, an identical 3 s fixation period also followed the presentation of the 2 questions after each trial. All responses were given using an MR-compatible response devise (Dancer Designs) with a single button and dial (50 mm diameter) response capability. The dial had 180° of rotation, where –90° corresponded to "extremely dissatisfied" and "strongly disagree" for the body satisfaction and body ownership questions, respectively, and +90° corresponded to "extremely satisfied" and "strongly agree." Participants rotated the dial to indicate their level of satisfaction/agreement and then registered each response by pressing the button. Each question was allocated a 6 s response time. To improve the accuracy of the responses, the 0° position was indicated by a plastic marker that the participant could feel when the dial was rotated to 0°. To check the reliability of the responses, 30 of the participants also provided additional baseline body satisfaction scores using a traditional visual analogue scale (VAS) just before entering the scanner. These VAS responses were found to correlate strongly with the baseline responses made with the dial in the scanner ($r = 0.616$, $n = 30$, $P < 0.001$). Before scanning commenced, all participants were required to familiarize themselves with the response device to ensure that they could respond within the 6 s time frame and were aware of the full rotation of the dial and the position of the button. After each trial block, there was a 20 s rest period (fixation cross). The experiment comprised 4 experimental runs, each consisting of 3 blocks of 4 trials and lasting 10 min and 6 s. Thus, the full experiment consisted of a total of 48 trials (12 per condition) with a complete scanning time of 40 min and 24 s. Between runs 2 and 3, a high-resolution anatomical scan was completed for coregistration (see details below). The anatomical scan was run at this time to give participants a break from the task, thereby reducing fatigue and the number of missed responses.

Functional Imaging Data Analysis

Functional brain images were collected using a 3 T TIM Trio MRI scanner (Siemens). fMRI makes use of blood-oxygenation level-dependent (BOLD) signals as an index of neural activity

with a relatively high spatial resolution (2–3 mm). BOLD-signal changes were recorded with a T2*-sensitive echo planar imaging pulse sequence (repetition time (TR) = 3 s; echo time (TE) 40 ms; flip angle 90°; 47 near-axial slices; 3 mm isotropic voxel size; matrix size 58 by 76, interleaved). Images were acquired using a 12-channel phased-array head coil. A high-resolution T1-weighted structural scan at 1 mm isotropic voxel size (voxel size = 1 mm × 1 mm × 1 mm, field of view = 256 mm × 256 mm, slices = 176, TR = 1900 ms, TE = 2.27 ms, flip angle = 9°) was also acquired for each subject for anatomical registration, segmentation, and display. Foam padding was used to stabilize each participant's head and to reduce motion artifacts.

All fMRI data preprocessing was completed using "Statistical Parametric Mapping Software 8," and fMRI data analysis was then completed using SPM12 (http//:www.fil.ion.ucl.ac.uk/spm; Wellcome Department of Cognitive Neurology, London). The functional images were motion-corrected with respect to the first volume in each series. Artifact detection tools were also used to ensure that there were no significant artifacts in the data. The images were also coregistered with the high-resolution structural scan and then normalized to Montreal Neurological Institute (MNI) standard reference space. In this normalization process, the functional images were resliced to a resolution of 2 mm × 2 mm × 2 mm and spatially smoothed with an 8 mm FWHM Gaussian kernel. For each experimental condition, we defined separate regressors to model each 30 s trial; the responses (15 s in total for the 2 questions and the subsequent 3 s of fixation) were modeled as separate conditions of no interest. The regressors were convolved with the standard hamodynamic response function modeled in SPM8. Contrasts of interest were computed for each participant at the single-subject level. These contrast images were then subjected to a random effects (second-level) general linear model (GLM) analysis (equivalent to a one-sample *t*-test). Because of our strong a priori hypotheses, only peaks surviving $P < 0.05$ significance level after familywise error corrections for multiple comparisons using a small volume correction were reported. For identification of these regions of interest, 10 mm spheres were created surrounding MNI coordinates from previous studies. For verification of illusion induction, we used coordinates in the premotor and intraparietal cortex that were reported from a full-body illusion by Petkova et al. (2011). For body satisfaction, we used coordinates previously associated with body anxiety in healthy participants and body satisfaction in anorexia patients in the right anterior insula (Friederich et al. 2010). For the anterior cingulate cortex, we used peaks from 3 separate studies with anorexia patients: coordinates from a region in the rostral anterior cingulate cortex associated with reduced activity in anorexia patients compared with controls during a body comparison task (Friederich et al. 2010); and 2 separate peaks in the dorsal anterior cingulate cortex associated with reduced gray matter volume (Joos et al. 2011) and reduced blood perfusion (Naruo et al. 2001) in patients with anorexia nervosa. In addition to these planned investigations, we also performed an exploratory whole-brain analysis and noted clusters of active voxels that survived $P < 0.05$ after false-discovery rate correction (see Supplementary Tables S2 and S3). For one female participant, 2 experimental blocks were removed from the analysis due to technical problems with fMRI images.

We used the contrast [(obese synchronous + slim synchronous) – (obese asynchronous + slim asynchronous)] to examine clusters of active voxels that were greater for the illusion (synchronous) conditions than for the 2 nonillusion control (asynchronous) conditions (main effect of synchrony). This main-effect contrast was also used for the regression analysis to correlate illusion-related neural activity against the equivalent behavioral measure (difference in illusion ratings between the synchronous and the asynchronous conditions). When investigating neural responses related to the affective responses that were triggered by illusory obesity, we examined the interaction term in the factorial design [(obese synchronous – obese asynchronous) – (slim synchronous – slim asynchronous), which we referred to as "interaction of timing × body type"]. This interaction contrast was also used when comparing males and females and in the regression analysis for evaluating the relationship between neural responses and eating-disorder psychopathology. For this analysis, we also entered BMI as a covariate of no interest.

To identify neural interactions between brain regions, we used psychophysiological interaction (PPI) analyzes. This method allows for identification of voxels in which activity is more related to activity in a seed region during a given psychological context, enabling the inference of effective connectivity between these brain areas. Thus, a seed region was identified in a key area—the right intraparietal cortex—involved in perceptual body illusions to determine whether its activity was related to the activity in areas associated with emotions during ownership of an obese body versus a slim body. First, a seed region was identified in the right intraparietal cortex using coordinates from a peak voxel described by Petkova et al. (2011) (the same peak as used for the regression analysis described above). We then created a mask that corresponded to a 6 mm sphere surrounding the local maxima peaks for each individual participant (De Martino et al. 2012; Schienle and Scharmüller 2013). The average time series for the seed region was then extracted and entered as a regressor for the GLM analysis, along with the interaction term (see above) as the psychological context. Small volume correction was applied in the anterior cingulate cortex and anterior insula cortex based on the same regions of interest as those used for the GLM analysis (as described above). For anatomical localization of the activations obtained in the different analyzes, we superimposed the activation maps onto the average normalized high-resolution MRI image of this group of participants and labeled using the nomenclature from a human brain atlas (Duvernoy et al. 1999). For brain areas with activations at $P < 0.001$ uncorrected for the main analyzes, see Supplementary Tables S2 and S3. These activations should be interpreted with caution but nevertheless provide descriptive information about the anatomical specificity of the effects.

Results

First, we examined the behavioral data to confirm illusion induction and modulation of body satisfaction. As expected, we found significantly higher ratings of body ownership for the synchronous versus asynchronous trials ($z = -4.92$, $P < 0.001$; see Table 2). Owning an obese body produced significantly lower body satisfaction compared with preillusion baseline scores ($z = -2.49$, $P = 0.013$) (Fig. 2), and females exhibited greater dissatisfaction than males ($z = -2.04$, $P = 0.043$) (Fig. 3). Unsurprisingly, ownership of a slim body did not significantly change body satisfaction in our predominantly normal-sized participants (max $z = -0.803$, $P = 0.422$), nor were differences in body satisfaction between the sexes observed under this condition ($z = -1.73$, $P = 0.086$). Thus, our approach to experimentally reduce body satisfaction by inducing illusory ownership over an obese body was successful (for further details, see "Additional Behavioral Results" section).

When evaluating the fMRI results, we first assessed activations associated with the perceptual body illusion in the fronto-parietal

Table 2 The medians (means and standard error in parentheses) of body ownership and body satisfaction for each experimental condition

Measure	Body	Score	Male median	Female median	Total median
Ownership	Obese	Synchronous	−14.2 (−8.3, 10.2)	−13.88 (−12.9, 9.5)	−14.2[a] (−10.9, 6.9)
		Asynchronous	−50.31 (−40.7, 11.0)	−40.55 (−36.7, 8.2)	−45.17 (38.7, 6.8)
		Score (sync–async)	24.9 (31.9, 7.6)	17.55 (23.7, 5.2)	24.59 (27.8, 4.6)
	Slim	Synchronous	33.95 (28.1, 9.4)	10.73 (0.58, 10.9)	17.62[a] (14.3, 7.5)
		Asynchronous	−27.64 (−9.2, 13.1)	−47.73 (−40.3, 11.2)	−37.83 (24.7, 8.9)
		Score (sync–async)	35.04 (37.2, 8.0)	45.57 (40.8, 9.3)	40.18 (39.0, 6.2)
Body satisfaction	Obese	Synchronous	53.71 (39.9, 10.6)	13.16[a] (15.1, 10.6)	41.78 (27.5, 7.7)
		Asynchronous	49.98 (39.1, 10.6)	15.72[a] (18.9, 10.6)	38.01[a] (28.9, 7.6)
		Score (sync–async)	0.18 (0.73, 0.9)	−4.12 (−3.73, 1.8)	−1.34 [a] (−1.5, 1.0)
	Slim	Synchronous	54.7 (49.2, 6.1)	21.68[a] (29.9, 8.4)	48.78 (39.5, 5.4)
		Asynchronous	56.36 (50.1, 6.3)	26.21[a] (29.7, 9.4)	51.99 (39.9, 5.8)
		Score (sync–async)	0.77 (−0.89, 1.3)	−0.37 (0.23, 2.1)	0.12[a] (−0.33, 1.2)
		Baseline	61.29 (53.8, 6.9)	44.36 (34.5, 10.9)	57.39[a] (44.4, 6.6)

[a]Data are normally distributed; all other data are non-normal (Shapiro–Wilk statistic $P < 0.05$).

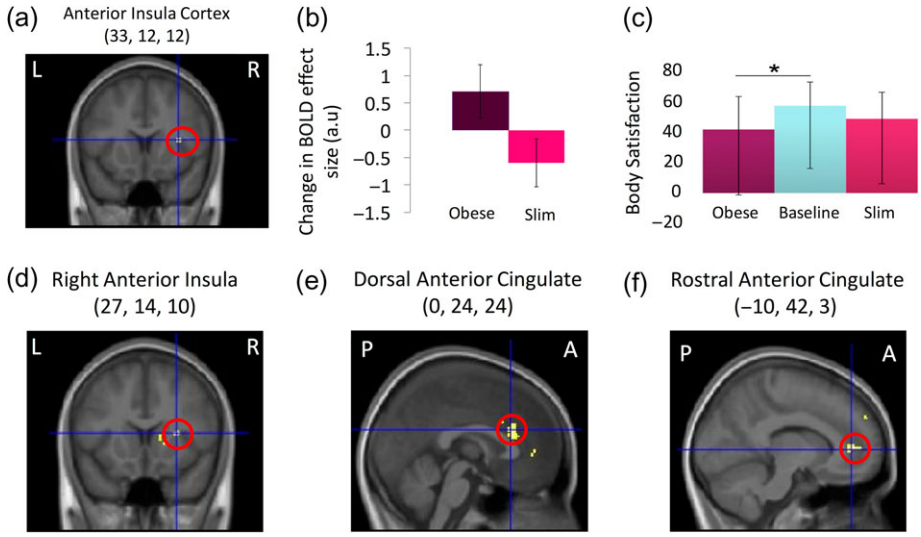

Figure 2. Neural and behavioral effects of illusory obesity: Ownership of an obese body resulted in greater activation in the right anterior insula cortex compared with ownership of a slim body (i.e., interaction timing × body type; *a* and *b*) and a significant reduction of rated body satisfaction relative to baseline (*c*). PPI analysis revealed effective connectivity related to illusory obesity between the intraparietal sulcus (seed) and active sections of the right anterior insula (*d*) and the dorsal (*e*) and rostral (*f*) anterior cingulate cortex. fMRI results are reported at $P < 0.05$ corrected in volumes of search space defined a priori. For display purposes, the activation maps were thresholded at $P < 0.001$ uncorrected and overlaid onto the average structural MR-scan of this sample. The graphs depict the means and standard errors for the contrast estimates of each of the 4 conditions compared with the resting baseline (*b*) and the medians and interquartile range of the body satisfaction ratings (*c*). L, R, P, and A denote left, right, posterior, and anterior, respectively.

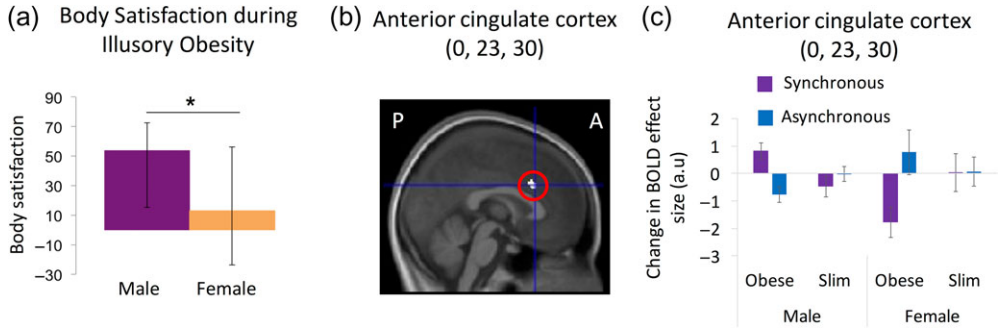

Figure 3. Sex Differences: Females reported significantly lower body satisfaction (*a*) and were found to have attenuated dorsal anterior cingulate activation during illusory obesity (interaction timing × body type in the factorial design) compared with males (*b*, *c*). The highlighted region corresponds to $P < 0.05$ corrected for multiple comparisons in search space defined a priori. For display purposes, the activation map was thresholded at $P < 0.001$ uncorrected and was overlaid onto the average structural MR-scan of this group of participants. The graphs depict the medians and interquartile range of the body satisfaction ratings (*a*) and the means and standard errors for the contrast estimates of each of the 4 conditions compared with the resting baseline for male and female participants (*c*). P and A denote posterior and anterior, respectively.

association areas related to multisensory integration of bodily signals, particularly in the ventral premotor cortex and the cortices lining the intraparietal sulcus in the posterior parietal lobe, which were identified in previous studies using emotionally neutral body illusions (Ehrsson et al. 2004; Ehrsson, Kito, et al. 2005; Petkova et al. 2011; Gentile et al. 2013; Guterstam, Björnsdotter, et al. 2015). To accomplish this, we compared the synchronous versus asynchronous conditions (across body type) and identified areas in which the amplitude of the resulting activation was systematically and positively related to the subjective vividness of the illusion. As expected, we found activations related to the illusion of owning the stranger's body in the bilateral ventral premotor cortex (right precentral gyrus, 48, 3, and 28, $t = 4.34$, $P = 0.01$ corrected; left precentral gyrus, −56, 5, and 28, $t = 4.03$, $P = 0.02$ corrected; the coordinates refers to x, y, and z in the standard space of the MNI) and in the anterior region of the cortex lining the right intraparietal sulcus (33, −49, and 51, $t = 4.22$, $P = 0.013$ corrected) (Fig. 4 and Supplementary Table S2). To ensure that these findings were not due to the presence of possible statistical outliers, we verified the results using a linear regression with a modified algorithm (Robustfit in MATLAB R2015a). This algorithm gives lower weighting to data points that do not fit well and, therefore, is much less susceptible to outliers (see Ehrsson et al., 2005). All identified peaks retained significance at $P < 0.05$ with this modified analysis (see Fig. 4). Moreover, in addition to our hypothesis-driven small volume correction, activity in the right precentral gyrus and the right intraparietal sulcus relating to illusion strength were both part of clusters that survived whole-brain cluster correction (see Supplementary Table S2). The explorative whole-brain analysis (see Supplementary Table S2) also revealed significant activations in other areas that are associated with body ownership illusions, such as the cerebellum (Ehrsson, Kito, et al. 2005; Petkova et al. 2011; Gentile et al. 2013; Guterstam et al. 2013), the putamen (Petkova et al. 2011), the frontal operculum (Ehrsson, Holmes, et al. 2005; Petkova et al. 2011) and the lateral occipital cortex (Petkova et al., 2011; Gentile et al., 2013; Guterstam et al., 2013, 2015; Limanowski and Blankenburg, 2015, 2016). Thus, the brain activation pattern we observed demonstrates that we successfully induced full-body illusions with the obese and slim models in the scanner environment (see Supplementary Table S2).

After this, we examined the neural basis of the obesity illusion-induced affective responses (i.e., the interaction term in the factorial design). Illusory ownership of an obese versus slim body led to increased activation in the right anterior insular cortex (significant interaction between timing and body type; 33, 12, and 12, $t = 3.7$; $P = 0.016$ corrected) (Fig. 2 and Supplementary Table S3). This finding supports our hypothesis that this region plays a role in body dissatisfaction. However, we did not observe activation of the anterior cingulate cortex as we had expected; this was probably due to the significant interindividual differences between the sexes that was revealed in a subsequent analysis (see below).

Next, we sought to determine how changes in affective body representation are functionally related to the perceptual experience of the body in the posterior parietal cortex. We found that that illusory obesity was associated with a significant increase in effective connectivity between the right intraparietal cortex and the right anterior insular cortex (27, 14, and 10, $t = 3.88$, $P = 0.033$ corrected), the dorsal anterior cingulate cortex (0, 24, and 24, $t = 3.99$, $P = 0.026$ corrected), and the rostral anterior cingulate cortex (−10, 42, and 3, $t = 4.28$, $P = 0.014$ corrected) (Fig. 2; PPI analysis using the right intraparietal cortex as a "seed region"; see "Materials and Methods" section). This provides evidence for functional interactions between perceptual and affective body representations, possibly suggesting that information about increases in body size reaches the anterior insula and the anterior cingulate cortex where it modifies body-related affective responses.

We then examined how individual differences in brain responses to perceived obesity relate to eating-disorder vulnerability. In a separate regression analysis, we found that levels of nonclinical eating-disorder psychopathology (EDE-Q score) predicted obesity illusion-induced activation at 2 foci in the dorsal anterior cingulate cortex (−6, 33, and 21, $t = 4.5$, $P = 0.008$

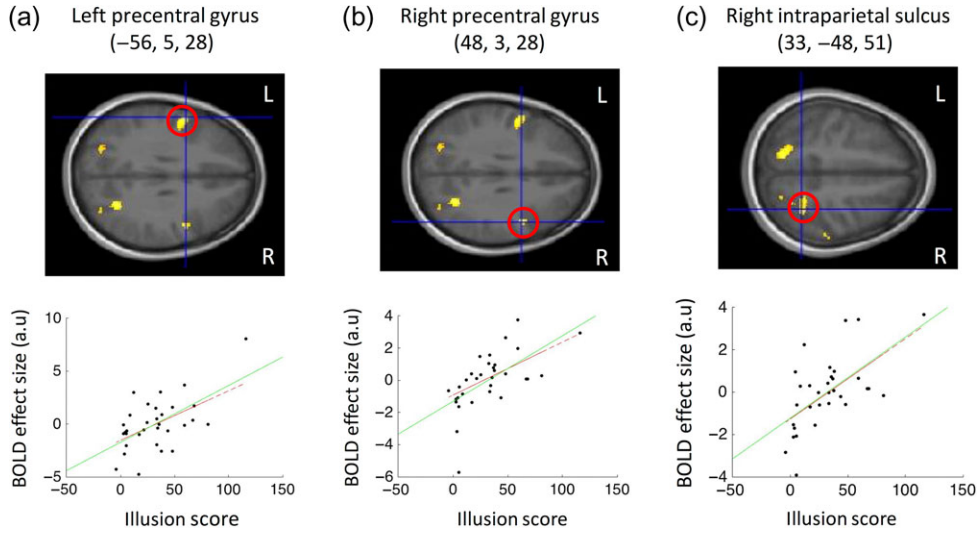

Figure 4. Activations reflecting illusory ownership of a stranger's body (irrespective of size): Ratings of body ownership (scored using a 180-point response dial) in the synchronous condition relative to the asynchronous condition (illusion score) related to activation of the left precentral gyrus (*a*), the right precentral gyrus (*b*), and the right intraparietal sulcus (*c*). These results were obtained by comparing synchronous and asynchronous conditions and then regressing the resulting effect size with the illusion score across participants (green line represents regression slope). For display purposes activation maps were thresholded at $P < 0.001$ uncorrected and overlaid onto the average structural MR-scan of this group of participants. All highlighted areas (red circles and scatterplots) survived correction for multiple comparisons in volumes of search space defined a priori ($P < 0.05$ small volume correction). Regressions remained significant with Robustfit (red dashed line), which is less susceptible to possible outliers (see "Results" section). L and R denote left and right, respectively.

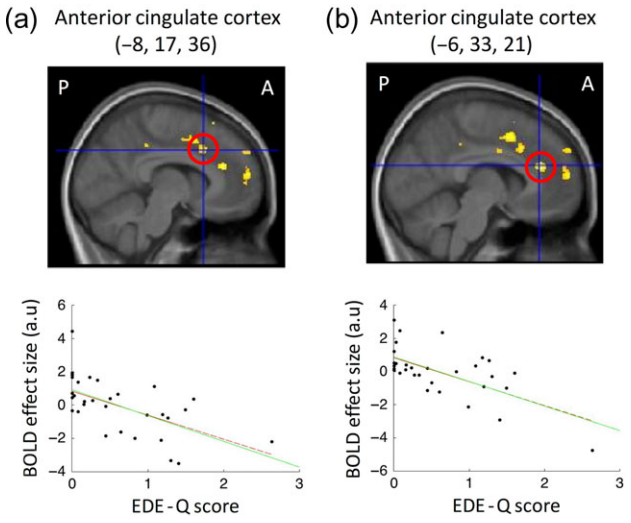

Figure 5. Neural correlates of eating-disorder vulnerability: Eating disorder psychopathology predicted neural responses related to owning an obese body at 2 foci in the dorsal anterior cingulate cortex (*a* and *b*): higher eating disorder psychopathology was associated with lower activation (interaction timing × body type in the factorial design). The highlighted regions correspond to $P < 0.05$ corrected for multiple comparisons in search spaces defined a priori (red circles and scatterplots). For display purposes, the activation maps were thresholded at $P < 0.001$ uncorrected and were overlaid onto the average structural MR-scan of this group of participants. Scatterplots show regression slope (green solid line) and Robustfit slope (red dashed lines). Regressions remain significant with Robustfit, which is less susceptible to possible outliers (see results). P and A denote posterior and anterior, respectively.

corrected; −8, 17, and 36, $t = 4.13$, $P = 0.019$ corrected) (Fig. 5 and Supplementary Table S3; systematically relating the EDE-Q score to the effect size of the interaction contrast across participants controlling for BMI; see "Materials and Methods" section). This observation provides evidence linking eating-disorder psychopathology to cingulate responsiveness during perceived changes in body size, such that higher eating-disorder psychopathology was associated with "lower" activation when owning an obese body. As before, these regression analyzes were confirmed using Robustfit, ensuring that the findings were not simply a result of possible outliers (see Fig. 5). Furthermore, in addition to our hypothesis-driven small volume correction, the activity in the anterior cingulate relating to eating-disorder vulnerability also survived whole-brain cluster correction (see Supplementary Table S3).

Finally, we explored possible sex-related differences in brain responses. Illusory ownership of an obese versus slim body (interaction of timing × body type) was associated with attenuation of neural response in the dorsal anterior cingulate cortex in females compared with males (0, 23, and 30; $t = 3.68$, $P = 0.045$ corrected) (Fig. 3). Thus, altered emotional responsiveness in the anterior cingulate cortex to perceived obesity might underlie eating-disorder vulnerability in females.

Additional Behavioral Results

Verification of the Illusion

For subjective responses, the mean synchronous score was calculated for each participant by collating their responses (one after each trial) to the ownership questions following the synchronous trials. These responses were then compared with the equivalent asynchronous responses using Wilcoxon signed-rank tests, as reported above. A nonparametric analysis was used because the asynchronous data were not normally distributed (Shapiro–Wilk statistic = 0.92, $P = 0.017$). An overall illusion score was calculated by subtracting the asynchronous responses from the synchronous responses, which was used in the regression analysis with brain images (see above and below for details).

Comparing ownership of the synchronous versus asynchronous trials for each body size condition revealed that synchronous touch resulted in higher levels of ownership compared with asynchronous touch for both obese ($z = -4.73$, $P < 0.001$) and slim ($z = -4.68$, $P < 0.001$) bodies. Further analysis revealed that the illusion score we used in the neuroimaging analysis (synchronous − asynchronous) was not significantly different between the 2 body types ($z = -1.76$, $P = 0.079$). This illusion score was also found to be statistically equivalent for males and females in both slim ($z = -0.188$, $P = 0.867$) and obese ($z = -0.452$, $P = 0.669$) body sizes. Nonparametric tests (Wilcoxon signed-rank and Mann–Whitney *U* for within and between analyzes, respectively) were used because the illusion scores and the responses in the asynchronous trials were non-normally distributed (maximum Shapiro–Wilk statistic = 0.93, $P = 0.036$). See Table 2 for descriptive statistics corresponding to each condition.

Body Satisfaction

To directly test our hypotheses that ownership of an obese body would decrease body satisfaction, the mean baseline rating scores were obtained by collating the responses given at the beginning of each experimental run and comparing this to the mean scores for each condition (collated across trials). One participant had to be omitted from this analysis because of failure to respond to any of the baseline body satisfaction questions. Only the baseline responses (Shapiro–Wilk statistic = 0.95, $P = 0.155$) and those following the obese asynchronous condition (Shapiro–Wilk statistic = 0.935, $P = 0.061$) were found to be normally distributed; therefore, this comparison was conducted using a paired sample *t*-test, which revealed no significant difference ($t(30) = -0.85$, $P = 0.074$). All other comparisons were completed using Wilcoxon signed-rank tests. Only the body satisfaction ratings in the obese-body synchronous conditions revealed a significant difference from baseline, as reported above (obese synchronous $z = -22.49$, $P = 0.013$; slim synchronous $z = -0.803$, $P = 0.422$; slim asynchronous $z = -0.666$, $P = 0.505$). All of the male responses were non-normally distributed (maximum Shapiro–Wilk statistic = 0.871, $P = 0.029$), whereas all female responses were normally distributed (minimum Shapiro–Wilk statistic = 0.935, $P = 0.325$). Therefore, nonparametric Mann–Whitney *U*-tests were used to test the hypothesized differences in body satisfaction between males and females at baseline and each separate condition (see Table 2). All the data were checked for statistical outliers (Iglewicz and Hoaglin 1993), and none were found.

Discussion

From a cognitive neuroscience perspective, this study yielded two important novel findings. First, affective feelings of body dissatisfaction are related to neural processing in the right anterior insular cortex and the anterior cingulate cortex, albeit the level of cingulate activity is modulated by sex differences and individual differences in eating-disorder vulnerability. Second, these affective body representation regions are functionally connected to the perceptual body representation in the posterior parietal cortex. Although PPI analysis does not demonstrate directionality, these results may imply that perceived

body size can directly influence feelings of body satisfaction through these interacting brain regions. This is important because it shows that the affective systems related to interoceptive awareness and monitoring our body's physiological well-being—the insular and anterior cingulate cortices—are functionally linked to the perceptual representation of one's own body in the posterior parietal cortex. The results are also clinically relevant because they implicate changes in the activity of the dorsal anterior cingulate cortex—a region previously associated with anorexia (Naruo et al. 2001; Friederich et al. 2010; Joos et al. 2011)—to eating-disorder psychopathology in healthy nonemaciated participants and to eating-disorder vulnerability in women (see further discussion below).

The observed activity in the premotor cortex and the right intraparietal cortex is consistent with earlier studies suggesting that full-body illusions occur through the integration of spatially and temporally congruent visual, tactile, and proprioceptive information, creating a coherent multisensory representation of a single owned body (Petkova et al. 2011; Gentile et al. 2015; Guterstam, Abdulkarim, et al. 2015). In nonhuman primates, these regions contain neurons that can integrate visual, tactile, and proprioceptive signals from space near the body at the single neuron-level (Rizzolatti et al. 1981; Andersen et al. 1997; Graziano et al. 1997, 2000), and neuroimaging studies have confirmed the existence of neuronal populations with similar response properties in the human premotor and intraparietal cortices (Ehrsson et al. 2004; Petkova et al. 2011; Brozzoli et al. 2012; Limanowski and Blankenburg 2015). Moreover, the cortex that lines the more anterior part of the intraparietal cortex is sensitive to changes in perceived waist size, as demonstrated in a previous fMRI body illusion experiment (Ehrsson, Kito, et al. 2005). Although earlier studies have shown how applying physical threat toward a body that feels like one's own triggers anxiety and neural responses in the anterior insula and anterior cingulate cortices (Ehrsson et al. 2007; Gentile et al. 2013), these studies did not investigate body dissatisfaction or changes in functional connectivity between these regions and the posterior parietal cortex. This study, therefore, expands on this and on previous affective neuroscience imaging studies (Friederich et al. 2007; Mohr et al. 2011; Castellini et al. 2013) by offering an explanation of how perceptual body representations in the posterior parietal cortex can directly influence body satisfaction in healthy individuals.

To the best of our knowledge, this study is the first to directly investigate the neural correlates of feelings of body dissatisfaction in healthy controls in relation to body perception. The results, implicating the right anterior insular cortex in both sexes and the anterior cingulate cortex in men (see further below), are consistent with the notion that these 2 structures are related to emotional processing (Damasio et al. 2000; Craig 2009; Etkin et al. 2011), and in particular, to negative emotions associated with various bodily reactions, such as pain, itch, cooling, anger, sadness, fear, disgust (Phillips et al. 1997; Damasio et al. 2000; Wicker et al. 2003; Mobbs et al. 2010), and interoceptive awareness (Craig 2002; Olausson et al. 2002; Critchley et al. 2004). Our results thus speculatively suggest that body dissatisfaction, as reported by participants, may constitute a homeostatic negative bodily emotion similar to pain, muscular fatigue, or disgust at the level of central neural representations. Finally, our results from the functional connectivity analysis revealed how the right anterior insular cortex and the anterior cingulate cortex might work in concert with the posterior parietal cortex to link the affective-emotional representations and spatial-perceptual representations of the body. This new observation may underscore the dynamic and interconnected nature of central body representations and could suggest that negative bodily emotions can be triggered from the posterior parietal cortex simply as a result of a perceptual body illusion without changes in afferent interoceptive signals from the body. Future studies should examine the possible bidirectionality of this interplay; in other words, they should investigate if changes in body satisfaction caused by cultural, social, or other environmental factors lead to changes in parietal activation and perceived body size.

A previous positron emission tomography study reported a correlation between a behavioral index of a limb ownership illusion—the so called "proprioceptive drift" [which measures the degree to which position sense of a limb is shifted toward the artificial hand during the rubber hand illusion (Botvinick and Cohen 1998)]—and regional cerebral blood flow in the left mid-posterior insular cortex (Tsakiris et al. 2007). In this study, we observed a cluster of active voxels in the frontal operculum close to the right anterior insula (see Supplementary Table S2) when inspecting the contrast for neural correlates of the basic body ownership illusion, but this was at a different location to the activation we observed associated with body dissatisfaction. Although there was no significant difference in the illusion scores between the different body sizes in this study, the difference did approach significance with a trend toward a stronger illusion for the slim body ($P = 0.07$). Thus, a critical reader could raise the concern that the activation of the right anterior insular cortex observed here, which we attributed to body dissatisfaction, could in fact reflect differences in the basic multisensory illusion of owning the stranger's body rather than emotional responses. However, we believe this notion is unlikely because such an ownership-related effect should be greater for the slim body compared with the obese body, and this is exactly the opposite from the pattern of responses we observed in the active section of the anterior insula that was associated with illusory obesity (Fig. 2*b*). However, future studies should investigate the underlying neural mechanisms associated with illusion nonresponders to identify possible networks associated with reduced rather than increased illusion scores. Examining the possibility of a negative relationship between BOLD responses and illusion scores in our results, we found no significant clusters in our search regions, including in the anterior insular.

A related concern is that the actual body size of the participant may have influenced illusion strength, which in turn may affect our imaging findings. This concern stems from the fact that most of our current sample were closer in actual body size BMI to the slim rather than the obese body, which conceivably could account for the trend of lower illusion scores for the obese body. However, we feel that it is very unlikely that this accounts for the main results given that we found no significant relationship between the illusion scores and BMI in this study (see Supplementary Table S1), nor did we find a significant relationship between the difference in BMI between the actual body and the model (which differs from BMI alone due to the differences in BMI between the male and female obese models) and the strength of the body ownership illusions (max $r = -0.177$, $P = 0.331$); neither BMI nor this difference in BMI changed the significant clusters in any of our results when used as a covariate of no interest, and no significant clusters were found in any of our a priori search spaces when searching for a linear relation between the difference in BMI and the activity related to illusory obesity (the interaction term) or a main effect of the illusion (synchronous – asynchronous across body types). Moreover, from previous studies, we know that

full-body illusions are robust to differences in the size and shape of bodies (Normand et al. 2011; van der Hoort et al. 2011; Preston and Newport 2012; Banakou et al. 2013; Preston and Ehrsson 2014). Thus, in our opinion, we can refute the concern that differences in BMI between the participants' actual bodies and the model bodies influenced the illusions and our imaging results (for similar arguments regarding eating-disorder psychopathology and cingulate activation, see below).

From a clinical perspective, the cingulate activity triggered by perceived obesity was related to eating-disorder psychopathology and was reduced in females compared with males. The anterior cingulate and anterior insula have previously been linked to anorexia nervosa, but physical effects of starvation complicate the interpretation of abnormal brain structure/activity in such samples, as it is not clear whether the observed abnormalities are related to pathology or the physical effects of starvation (Frank 2013). Therefore, our results may have important clinical relevance because they implicate anterior cingulate activity in eating-disorder psychopathology in healthy, nonemaciated participants. Our findings also suggest that the reason women are more vulnerable to developing eating disorders compared with men is due to a lower dorsal anterior cingulate response to perceived obesity. It is possible that the reduced anterior cingulate activity observed in females is purely a consequence of females having higher eating-disorder psychopathology, as, although there was no significant difference in EDE-Q scores between our male and female participants, this did approach significance (see Table 1) and, reduced activity was found in 2 activation peaks in the anterior cingulate cortex for high eating-disorder psychopathology close to the single peak observed when comparing females versus males. Reanalysing the male versus female contrast while controlling for the level of eating-disorder psychopathology resulted in the relative deactivation within the anterior cingulate cluster to no longer reach significance. However, it is impossible to determine whether women may have lower activity in the anterior cingulate because they have higher eating-disorder psychopathology or whether they have higher eating-disorder psychopathology because they have lower activity in the anterior cingulate. Future research should expand from these results to try to understand more about eating-disorder vulnerability and the role of the anterior cingulate.

One possible explanation for the observed anterior cingulate activity in this experiment is via emotion regulation mechanisms. It has been suggested that the dorsal part of the anterior cingulate cortex, the region identified in this study, is important for mechanisms associated with cognitive regulation of emotion (an ability that is impaired in anorexia; Oldershaw et al., 2015) rather than emotional expression per se (Bush et al. 2000). Thus, the reduced dorsal cingulate activity observed here in women and in those with higher eating-disorder psychopathology (regression analysis) may therefore reflect a vulnerability to eating disorders due to a reduced ability of the dorsal anterior cingulate cortex to regulate emotions directed toward the body.

However, the anterior cingulate cortex has also been implicated in other mechanisms, including conflict monitoring. Therefore, an alternate explanation for the pattern of activity we observed in the anterior cingulate is that it reflects detection of a conflict between the participant's own body and that of the owned obese body. However, it is unlikely that such activity reflects a crude conflict in body size. We did not observe activation in the anterior cingulate when analyzing the basic effect of owning the obese and slim bodies, which is in line with previous full-body illusion studies that also involve conflict between an owned stranger's body and one's actual body, and do not report activity within the anterior cingulate (e.g., Guterstam, Björnsdotter, et al. 2015). Furthermore, an additional analysis using a measure of the difference in BMI between the participants' actual bodies and the model as a covariate of no interest revealed the same significant clusters in the anterior cingulate cortex as the original analysis of nonclinical eating-disorder psychopathology. Finally, regressing this difference in BMI measure against the brain activity related to illusory obesity (the interaction term) revealed no significant clusters in any of the a priori search spaces, which means that none of these areas seem to signal "conflict error" between illusory and actual body sizes.

It may be conceivable that conflicts are detected that are not captured by actual differences in body size. As stated above, patients with eating disorders, particularly anorexia nervosa, are thought to have deficits in the way they experience their own body, specifically by overestimating their actual body size (Slade and Russell 1973; Keizer et al. 2013). This body size overestimation may therefore also be apparent, albeit to a lesser extent, for those with higher eating-disorder psychopathology in the healthy population. Thus, these individuals may experience less of a conflict with the obese body (and therefore exhibit reduced activity in the anterior cingulate) irrespective of actual differences in body size because they do not have a true veridical experience of their own body. Such an explanation of conflict monitoring is not necessarily incompatible with explanations of emotion regulation. It has been suggested that the detection of conflicts in the anterior cingulate is essential for cognitive control processing (Carter and Veen 2007). Thus, detecting a discrepancy between one's actual body and what one knows/thinks about his/her actual body size may be an integral part of the mechanisms involved in regulating resultant emotional responses. However, body size distortions in anorexia are still debated (Cornelissen et al. 2013), and overestimations of body size among healthy participants are even less studied, so this explanation remains speculative. Despite this uncertainty regarding the mechanisms underlying the link between cingulate activity and eating-disorder psychopathology, demonstrating this link in individuals with healthy brains adds further clinical relevance to future studies that aim to shed light on these important questions.

In sum, illusory feelings of obesity resulted in lower levels of reported body satisfaction, particularly in females, and were linked to activity in the anterior insula and the anterior cingulate cortex. Effective neural connectivity was found between these affective body representation regions and the neural representations of perceived body size in the posterior parietal cortex. Thus, the results of this study support a direct neural link between perceptual and affective body representations in the brain. Moreover, cingulate neural responses during illusory obesity were reduced in females and in those with high levels of nonclinical eating-disorder psychopathology, which may relate this region to eating-disorder vulnerability. Importantly, because these current data connect activity in the anterior cingulate to eating-disorder psychopathology in healthy samples, this may suggest that abnormalities in structure or function observed previously in this region in anorexia patients may be linked to the pathology of the disease rather than being a consequence of starvation. Therefore, in addition to these results revealing how perceptual and affective body representations interact in the human brain, they may also help to explain the neurobiological underpinnings of eating-disorder vulnerability in women.

Supplementary Material

Supplementary material can be found at: http://www.cercor.oxfordjournals.org/

Funding

The James S. McDonnell Foundation, Torsten Söderbergs Stiftelse Vetenskapsrådet, and Hjärnfonden. The Wenner-Gren Foundations and Marie Curie Actions (to C.P.).

Notes

We acknowledge Giovanni Gentile and Pawel Tacikowski for technical advice on the SPM analyzes and Andreas Kalckert, Hiske van Duinen, Lorextu Bergunian, and Claudio Brozzoli for assistance with operating the MRI scanner. All fMRI experiments took place at Karolinska University Hospital, Huddinge. *Conflict of Interest*: None declared.

References

Andersen RA, Snyder LH, Bradley DC, Xing J. 1997. Multimodal representation of space in the posterior parietal cortex and its use in planning movements. Annu Rev Neurosci. 20: 303–330.

Banakou D, Groten R, Slater M. 2013. Illusory ownership of a virtual child body causes overestimation of object sizes and implicit attitude changes. Proc Natl Acad Sci USA. 110: 12846–12851.

Botvinick M, Cohen J. 1998. Rubber hands "feel" touch that eyes see. Nature. 391:756.

Brozzoli C, Gentile G, Ehrsson HH. 2012. That's near my hand! Parietal and premotor coding of hand-centered space contributes to localization and self-attribution of the hand. J Neurosci. 32:14573–14582.

Bush G, Luu P, Posner M. 2000. Cognitive and emotional influences in anterior cingulate cortex. Trends Cogn Sci. 4: 215–222.

Carter CS, Veen V. 2007. Anterior cingulate cortex and conflict detection: an update of theory and data. Cogn Affect Behav Neurosci. 7:367–379.

Castellini G, Polito C, Bolognesi E, D'Argenio A, Ginestroni A, Mascalchi M, Pellicanò G, Mazzoni LN, Rotella F, Faravelli C, et al. 2013. Looking at my body. Similarities and differences between anorexia nervosa patients and controls in body image visual processing. Eur Psychiatry. 28:427–435.

Cornelissen PL, Johns A, Tovée MJ. 2013. Body size overestimation in women with anorexia nervosa is not qualitatively different from female controls. Body Image. 10: 103–111.

Craig AD. 2002. How do you feel? Interoception: the sense of the physiological condition of the body. Nat Rev Neurosci. 3: 655–666.

Craig AD. 2009. How do you feel now? The anterior insula and human awareness. Nat Rev Neurosci. 10:59–70.

Critchley HD, Wiens S, Rotshtein P, Ohman A, Dolan RJ. 2004. Neural systems supporting interoceptive awareness. Nat Neurosci. 7:189–195.

Damasio AR, Grabowski TJ, Bechara A, Damasio H, Ponto LL, Parvizi J, Hichwa RD. 2000. Subcortical and cortical brain activity during the feeling of self-generated emotions. Nat Neurosci. 3:1049–1056.

De Martino B, Fleming SM, Garrett N, Dolan RJ. 2012. Confidence in value-based choice. Nat Neurosci. 16:105–110.

Duvernoy HM, Cabanis EA, Bourgouin P. 1999. The human brain: surface, three-dimensional sectional anatomy with MRI, and blood supply. New York: Springer.

Ehrsson HH, Holmes NP, Passingham RE. 2005. Touching a rubber hand: feeling of body ownership is associated with activity in multisensory brain areas. J Neurosci. 25:10564–10573.

Ehrsson HH, Kito T, Sadato N, Passingham RE, Naito E. 2005. Neural substrate of body size: illusory feeling of shrinking of the waist. PLoS Biol. 3:1–8.

Ehrsson HH, Spence C, Passingham RE. 2004. That's my hand! Activity in premotor cortex reflects feeling of ownership of a limb. Science. 305:875–877.

Ehrsson HH, Wiech K, Weiskopf N, Dolan RJ, Passingham RE. 2007. Threatening a rubber hand that you feel is yours elicits a cortical anxiety response. Proc Natl Acad Sci USA. 104: 9828–9833.

Etkin A, Egner T, Kalisch R. 2011. Emotional processing in anterior cingulate and medial prefrontal cortex. Trends Cogn Sci. 15: 85–93.

Fairburn CG, Harrison PJ. 2003. Eating disorders. Lancet. 361: 407–416.

Frank GKW. 2013. Altered brain reward circuits in eating disorders: chicken or egg? Curr Psychiatry Rep. 15:396.

Friederich H-C, Brooks S, Uher R, Campbell IC, Giampietro V, Brammer M, Williams SCR, Herzog W, Treasure J. 2010. Neural correlates of body dissatisfaction in anorexia nervosa. Neuropsychologia. 48:2878–2885.

Friederich H-C, Uher R, Brooks S, Giampietro V, Brammer M, Williams SCR, Herzog W, Treasure J, Campbell IC. 2007. I'm not as slim as that girl: neural bases of body shape self-comparison to media images. Neuroimage. 37:674–681.

Gentile G, Björnsdotter M, Petkova VI, Abdulkarim Z, Ehrsson HH. 2015. Patterns of neural activity in the human ventral premotor cortex reflect a whole-body multisensory percept. Neuroimage. 109:328–340.

Gentile G, Guterstam A, Brozzoli C, Ehrsson HH. 2013. Disintegration of multisensory signals from the real hand reduces default limb self-attribution: an fMRI study. J Neurosci. 33:13350–13366.

Gentile G, Petkova VI, Ehrsson HH. 2011. Integration of visual and tactile signals from the hand in the human brain: an FMRI study. J Neurophysiol. 105:910–922.

Graziano MSA. 1999. Where is my arm? The relative role of vision and proprioception in the neuronal representation of limb position. Proc Natl Acad Sci. 96:10418–10421.

Graziano MSA, Cooke DF, Taylor CSR. 2000. Coding the location of the arm by sight. Science. 290:1782–1786.

Graziano MSA, Hu XT, Gross CG. 1997. Visuospatial properties of ventral premotor cortex . J Neurophysiol. 77:2268–2292.

Grogan S. 2008. Body Image: Understanding Body Dissatisfaction in Men, Women, and Children. 2nd ed. New York: Routledge.

Guterstam A, Abdulkarim Z, Ehrsson HH. 2015. Illusory ownership of an invisible body reduces autonomic and subjective social anxiety responses. Sci Rep. 5:9831.

Guterstam A, Björnsdotter M, Gentile G, Ehrsson HH. 2015. Posterior cingulate cortex integrates the senses of self-location and body ownership. Curr Biol. 25:1416–1425.

Guterstam A, Gentile G, Ehrsson HH. 2013. The invisible hand illusion: multisensory integration leads to the embodiment of a discrete volume of empty space. J Cogn Neurosci. 25:1078–1099.

Iglewicz B, Hoaglin DC. 1993.How to detect and handle outliers, 16. Milwaukee, WI: ASQC Quality Press.

Joos A, Hartmann A, Glauche V, Perlov E, Unterbrink T, Saum B, Tüscher O, Tebartz van Elst L, Zeeck A. 2011. Grey matter deficit in long-term recovered anorexia nervosa patients. Eur Eat Disord Rev. 19:59–63.

Keizer A, Smeets MAM, Dijkerman HC, Uzunbajakau SA, van Elburg A, Postma A. 2013. Too fat to fit through the door: first evidence for disturbed body-scaled action in anorexia nervosa during locomotion. PLoS One. 8:e64602.

Keizer A, Smeets MAM, Dijkerman HC, van den Hout M, Klugkist I, van Elburg A, Postma A. 2011. Tactile body image disturbance in anorexia nervosa. Psychiatry Res. 190:115–120.

Lawler M, Nixon E. 2011. Body dissatisfaction among adolescent boys and girls: the effects of body mass, peer appearance culture and internalization of appearance ideals. J Youth Adolesc. 40:59–71.

Lecrubier Y, Sheehan DV, Weiller E, Amorim P, Bonora I, Sheehan KH, Dunbar GC. 1997. The mini international neuropsychiatric interview (MINI). A short diagnostic structured interview : reliability and validity according to the CIDI. Eur Psychiatry. 12:224–231.

Limanowski J, Blankenburg F. 2015. Network activity underlying the illusory self-attribution of a dummy arm. Hum Brain Mapp. 36:2284–2304.

Limanowski J, Blankenburg F. 2016. Integration of visual and proprioceptive limb position information in human posterior parietal, premotor, and extrastriate cortex. J Neurosci. 36: 2582–2589.

Mobbs D, Yu R, Rowe JB, Eich H, FeldmanHall O, Dalgleish T. 2010. Neural activity associated with monitoring the oscillating threat value of a tarantula. Proc Natl Acad Sci. 107:20582–20586.

Mohr HM, Röder C, Zimmermann J, Hummel D, Negele A, Grabhorn R. 2011. Body image distortions in bulimia nervosa: investigating body size overestimation and body size satisfaction by fMRI. Neuroimage. 56:1822–1831.

Mond JM, Myers TC, Crosby RD, Hay PJ, Rodgers B, Morgan JF, Lacey JH, Mitchell JE. 2008. Screening for eating disorders in primary care : EDE-Q versus SCOFF. Behav Res Ther. 46:612–622.

Naruo T, Nakabeppu Y, Deguchi D, Nagai N, Tsutsui J, Nakajo M, Nozoe S. 2001. Decreases in blood perfusion of the anterior cingulate gyri in anorexia nervosa restrictors assessed by SPECT image analysis. BMC Psychiatry. 1:2.

Normand J-M, Giannopoulos E, Spanlang B, Slater M. 2011. Multisensory stimulation can induce an illusion of larger belly size in immersive virtual reality. PLoS One. 6:e16128.

Olausson H, Lamarre Y, Backlund H, Morin C, Wallin BG, Starck G, Ekholm S, Strigo I, Worsley K, Vallbo AB, et al. 2002. Unmyelinated tactile afferents signal touch and project to insular cortex. Nat Neurosci. 5:900–904.

Oldershaw A, Lavender T, Sallis H, Stahl D, Schmidt U. 2015. Emotion generation and regulation in anorexia nervosa: a systematic review and meta-analysis of self-report data. Clin Psychol Rev. 39:83–95.

Petkova VI, Björnsdotter M, Gentile G, Jonsson T, Li T-Q, Ehrsson HH. 2011. From part- to whole-body ownership in the multisensory brain. Curr Biol. 21:1118–1122.

Petkova VI, Ehrsson HH. 2008. If I were you: perceptual illusion of body swapping. PLoS One. 3:e3832.

Phillips ML, Young AW, Senior C, Brammer M, Andrew C, Calder AJ, Bullmore ET, Perrett DI, Rowland D, Williams SCR, et al. 1997. A specific neural substrate for perceiving facial expressions of disgust. Nature. 389:495–498.

Pingitore R, Spring B, Garfield D. 1997. Gender differences in body satisfaction. Obes Res. 5:402–409.

Preston C, Ehrsson HH. 2014. Illusory changes in body size modulate body satisfaction in a way that is related to nonclinical eating disorder psychopathology. PLoS One. 9:e85773.

Preston C, Newport R. 2012. How long is your arm? Using multisensory illusions to modify body image from the third person perspective. Perception. 41:247–249.

Rizzolatti G, Scandolara C, Matelli M, Gentilucci M. 1981. Afferent properties of periarcuate neurons in macaque monkeys. I. Somatosensory responses. Behav Brain Res. 2:125–146.

Schienle A, Scharmüller W. 2013. Cerebellar activity and connectivity during the experience of disgust and happiness. Neuroscience. 246:375–381.

Slade PD, Russell GF. 1973. Awareness of body dimensions in anorexia nervosa: cross-sectional and longitudinal studies. Psychol Med. 3:188–199.

Smeets M a M. 1999. Body size categorization in anorexia nervosa using a morphing instrument. Int J Eat Disord. 25: 451–455.

Stice E, Shaw HE. 2002. Role of body dissatisfaction in the onset and maintenance of eating pathology: a synthesis of research findings. J Psychosom Res. 53:985–993.

Tsakiris M, Hesse MD, Boy C, Haggard P, Fink GR. 2007. Neural signatures of body ownership: a sensory network for bodily self-consciousness . Cereb Cortex. 17:2235–2244.

van der Hoort B, Guterstam A, Ehrsson HH. 2011. Being barbie: the size of one's own body determines the perceived size of the world. PLoS One. 6:e20195.

Wagner A, Ruf CAM, Braus DF, Schmidt MH. 2003. Neuronal activity changes and body image distortion in anorexia nervosa. Neuroreport. 14:2193–2197.

Wicker B, Perrett DI, Baron-Cohen S, Decety J. 2003. Being the target of another's emotion: a PET study. Neuropsychologia. 41:139–146.

Table S1: Correlation table showing correlations between the illusion scores for the obese and slim bodies with individual differences in body mass index (BMI), eating disorder psychopathology (EDE-Q), and self-esteem (SE). P values are adjusted to correct for multiple comparisons based on false discovery rate. * denotes significant differences.

	BMI	EDE-Q	SE	Obese	Slim
BMI					
Coefficient		.48	.129	-.041	-.347
p value		.619	.633	.823	.225
EDE-Q					
Coefficient	.48		.-156	.159	-.05
p value	.619		.619	.619	.823
SE					
Coefficient	.129	.-156		-.3	-.151
p value	.633	.619		.380	.619
Obese					
Coefficient	-.041	.159	-.3		.51
p value	.823	.619	.380		.03*
Slim					
Coefficient	-.347	-.05	-.151	.51	
p value	.225	.823	.619	.03*	

Table S2: Brain activations for the main effect of synchrony [(obese synchronous + slim synchronous) - (obese asynchronous + slim asynchronous)] and the regression analysis (main effect of synchrony with illusion score). These results are from the explorative whole-brain analysis, clusters containing peaks identified from the small volume correction are also listed (#).

Anatomical Region	Hemisphere	MNI x, y, z	Cluster size	t value
Main effect of synchrony (synchronous - asynchronous across body type)				
Intraparietal sulcus	R	28, -66, 45**	2202	4.96
Intraparietal sulcus	L	-20, -63, 37**	662	4.51
Cerebellum simple lobule	R	30, -67, -32	115	3.98
Lateral occipital sulcus	R	45, -58, -6*	139	3.84
Regression analysis (illusion score with main effect of synchrony)				
Lateral occipital sulcus	L	-33, -78, 9**	1096	6.08
Inferior frontal gyrus (frontal operculum)	R	40, 24, 3*	138	5.80
Parieto-occipital sulcus	R	28, -61, 26**	249	5.68
Lateral occipital sulcus	R	51, -58, 0**	930	5.67
Cerebellum lateral hemisphere	R	14, -58, -45**	324	5.38
Superior parietal gyrus	L	-16, -66, 52**	465	5.06
Cerebellum lateral hemisphere	R	38, -52, -35	116	4.98
Intraparietal sulcus	R	33, -36, 37*	93	4.90
Middle occipital gyrus, superior part	L	-26, -76, 34**	280	4.70
Putamen	R	30, -18, 4	97	4.70
Postcentral gyrus	R	57, -27, 46	75	4.69
Precentral gyrus (PMv)	L	-52, 2, 28$^{\#}$	188	4.68
Posterior transverse collateral sulcus	L	-33, -70, -9**	356	4.61
Intraparietal sulcus	R	33, -49, 54$^{\#}$**	360	4.54
Fusiform gyrus	R	40, -46, -20**	367	4.49
Precentral gyrus (PMv)	R	48, 3, 28$^{\#}$*	135	4.34

For descriptive purposes, all brain regions with activations at $p < .001$ uncorrected and a minimum cluster size of 20 are listed. Clusters containing activations that survived FWE correction for multiple comparisons in the a priori-defined small volumes of interest and FDR corrected clusters in the whole brain space are indicated: $^{\#}$= .05 peak level FWE small volume corrected; * = $p < .005$ FDR-corrected cluster level whole-brain, ** = $p < .001$ FDR-corrected whole-brain cluster level. Note that the peak coordinates from whole-brain analysis that is listed in this table can deviate slightly from the small volume correction analysis reported in the main text and figures.

Abbreviations: PMv = ventral premotor cortex. FDR = False discovery rate. FEW = Family wise error.

Table S3: Brain activations for the interaction [(obese synchronous - obese asynchronous) - (slim synchronous - slim asynchronous)) and regression analyses (interaction with EDE-Q controlling for BMI). These results are from the explorative whole-brain analysis, clusters containing peaks identified from the small volume correction are also listed (#).

Anatomical Region	Hemisphere	MNI x, y, z (mm)	Cluster size	t value
Interaction effect [(obese synchronous - obese asynchronous) - (slim synchronous - slim asynchronous)]				
Circular insula sulcus (AIC)	R	33, 11, 13#	47	4.20
Cerebellum lateral hemisphere	R	14, -51, -27	81	4.01
Superior precentral sulcus (PMv)	L	-32, -1, 36	34	3.85
Middle frontal gyrus	R	30, 47, 37	44	3.81
Regression analysis (interaction effect with EDE-Q score)				
Cerebellum lateral hemisphere	R	27, -66, -17**	283	6.16
Superior frontal gyrus	L	-14, 26, 61	77	5.19
Circular insula gyrus (AIC)	R	28, 12, 1	464	5.17
Superior frontal gyrus (SMA)	R	9, 8, 49**	748	5.16
Postcentral gyrus	L	-58, -28, 19*	220	5.05
Superior temporal sulcus	L	-45, -34, 1	54	4.90
Frontal gyrus (pars opercularis)	L	-48, -4, 3*	63	4.89
Caudate	R	6, 11, 6	52	4.67
Cingulate gyrus (ACC)	L	-8, 34, 21#	212	4.67
Superior frontal sulcus	R	15, 51, 33	110	4.65
Parietal operculum	L	-44, 8, -6	224	4.65
Middle frontal gyrus	L	-28, 41, 34**	159	4.58
Superior frontal sulcus	L	-12, 47, 39	225	4.43
Superior temporal gyrus	R	66, -12, 3	65	4.40
Postcentral gyrus	R	62, -21, 25	296	4.36
Frontal superior medial gyrus	L	-8, 58, 12	32	3.99
Cingulate gyrus (ACC)	L	-8, 17, 36#**	319	3.63

For descriptive purposes, all brain regions with significant activations at p <. 001 uncorrected and a minimum cluster size of 20 are listed. Clusters containing activations that survived FWE correction for multiple comparisons in the a priori-defined small volumes of interest and FDR corrected clusters in the whole brain space are indicated: #= .05 small volume-corrected peak level FWE; * = p < .005 FDR-corrected whole-brain cluster level, ** = p < .001 FDR corrected whole-brain cluster level. Note that the peak coordinates from whole-brain analysis that is listed in this table can deviate slightly from the small volume correction analysis reported in the main text and figures.

Abbreviations: PMv = ventral premotor cortex; SMA = supplementary motor cortex; ACC = anterior cingulate cortex; AIC = anterior insular cortex; EDE-Q = Eating Disorder Examination Questionnaire (eating disorder psychopathology); BMI = body mass index. FDR = false discovery rate; FEW = family wise error.